Hydrodynamics Laboratory
Kármán Laboratory of Fluid Mechanics and Jet Propulsion
California Institute of Technology
Pasadena, California

MEASUREMENTS ON FULLY WETTED AND VENTILATED RING WING HYDROFOILS

Department of the Navy, Bureau of Naval Weapons
Fluid Mechanics and Flight Dynamics Branch
Contract Nonr 220(54)

A. J. Acosta

E. R. Bate, Jr.

and

T. Kiceniuk

Report No. E-138.1

June 1965

ABSTRACT

Force measurements and visual observations were made in a water tunnel on fully wetted and ventilated flows past a family of conical ring wings having a flat plate section geometry. The diameter-chord ratio was varied from one to three, and the total included cone angle was 12 degrees. The fully wetted flows all exhibited separation from the leading edge except for the largest diameter-chord ratio, a result which was in agreement with previous work. The effect of ventilation is to reduce markedly the lift curve slope. Pressure distribution measurements were also made under ventilating conditions for one member of this series. The effect of ventilation over only a portion of the circumference of the ring was also briefly investigated. Large cross forces were developed by such ventilation and some comparisons are made between this method of obtaining control forces and more conventional methods.

LIST OF SYMBOLS

A	area, total wetted area of ventilating models, one-half wetted area of fully wetted models
A_T	cross-sectional area of torpedo
c	model chord (measured along cone generator)
C_D	drag coefficient $\frac{D}{1/2\,\rho V^2 A}$
C_L	lift coefficient $\frac{L}{1/2\,\rho V^2 A}$
$C_{L\alpha}$	rate of change of lift coefficient with angle of attack (radians)
C_M	moment coefficient $\frac{M}{1/2\,\rho V^2 A\,(2r_1)}$
C_{M_T}	torpedo moment coefficient $\frac{L\,\ell'}{1/2\,\rho V^2 A_T\,\ell}$
C_n	normal force coefficient $\frac{n}{1/2\,\rho V^2 \frac{A}{2\pi}}$
C_p	pressure coefficient $\frac{p - p_\infty}{1/2\,\rho V^2}$
C_Q	air flow rate coefficient $\frac{Q}{\pi (r_1^2 - r_2^2) V}$
D	total drag force
d	depth of model centerline from water surface
F	Froude number $\frac{V}{\sqrt{2\,g\,r_1}}$

LIST OF SYMBOLS (continued)

k	ventilation number $\frac{p_\infty - p_k}{1/2 \rho V^2}$
L	total lift force
ℓ	prototype torpedo length
ℓ'	distance from torpedo center of gravity to shroud ring leading edge
M	pitch moment about ring leading edge
n	normal force perpendicular to surface of conical ring per unit polar angle
N	total force perpendicular to ring axis
p	static pressure measured at any point of body
p_k	cavity pressure
p_∞	free-stream pressure far upstream of the model centerline
Q	quantity of ventilating gas supplied at ambient pressure in the cavity
r	radius measured to any point on the model measured from the model centerline
r_1	radius at entrance of ring
r_2	radius at exit of ring
$\frac{2r_1}{c}$	model aspect ratio
V	velocity
X	total chord force (along ring axis)
x	distance of pressure tap location from leading edge of model
α	angle of attack of force model

LIST OF SYMBOLS (continued)

γ	half cone angle of conical models (6 degrees)
θ	polar angle measured positive clockwise looking downstream from the water surface
ρ	water density

MEASUREMENTS ON FULLY WETTED AND VENTILATED RING WING HYDROFOILS

I. Introduction

The present report describes a series of experiments on a family of simple conical ring wings in fully wetted and ventilating flow. The general characteristics of ring wings in uniform flow are well known. Ring wings have found application in marine propellers, aircraft, underwater bodies such as torpedoes, and depth bombs. The function and description of many of these applications are to be found in Reference 1. The general theoretical background of ring wings is dealt with in References 2 through 9. A typical and somewhat historical application of ring wings to a torpedo is given in Reference 10.

All of the foregoing references and applications are concerned with fully wetted flow. That is, the fluid is either all liquid or all air. Because of the proximity of a neighboring free surface in a flow of liquid or perhaps by the deliberate injection of gas into a liquid flow, a two-phase flow may take place. The cavity of gas so formed may occupy only a portion of the boundary of the body so affected, in which case it is called partly cavitating (or partly ventilating if a supply of air is the cause of the cavity), or the cavitating or ventilating region may entirely surround the body except near the nose. In this case the flow is called supercavitating or superventilating.* The object of the present work is to study and to treat experimentally some of the problems arising with superventilating and partly ventilating ring wings.

Interest in these problems is due to the fact that this subject has great intrinsic value and is a nearly unexplored field of practical

*The words "ventilating" and "cavitating" are often used interchangeably in the literature and although ventilating is to be preferred when the cavities are air-supported, both terms are often used to describe this type of flow.

and theoretical treatment. This interest is also stimulated by the possibility of devising new schemes of force control which might augment or replace altogether the conventional rudders found on ships or possibly such devices as torpedoes which commonly employ a ring tail. The possibility of such an application was originally suggested by K. Smith and was followed up in the work of Lang and Daybell (Reference 11), in which water tunnel tests were carried out at the California Institute of Technology on normally fully wetted two-dimensional hydrofoils. Air was injected at various points on the hydrofoil, and it was observed that the resulting forces on the hydrofoil were greatly altered.

Few experimental or theoretical results on ventilating or cavitating flow past ring wings seem to be available. The only theoretical work known to the authors is an analytical study carried out with the aid of the rheo-electric analogy on the axisymmetric cavitating flow past a ring wing (Reference 12). In this work, use is made of linearized free streamline theory in setting up the approximations of the analogy. Several interesting examples are given in which the ring cross-sectional profile consists of straight line segments. All of these examples, however, have the pressure surface of the ring wing on the outside of the ring; the cavity that is thereby formed thus lies on the inside of the ring rather than the outside. The flow within the ring is therefore accelerated - as in a Kort nozzle - and not retarded, as would be more typical of shrouded propeller and pump-jet practice. The results in Reference 12 are not therefore directly applicable to these configurations and, being the results of an analogy, are not readily capable of generalization.

With these factors in mind it was decided to study the ventilated flow past ring wings using primarily an experimental approach. In application, the ring wing would almost certainly be used in conjunction with another body - such as a propeller shaft or hub - or it may be near another object, such as the hull of a ship as is treated in Reference 7. It was decided to begin by studying

MEASUREMENTS ON FULLY WETTED AND VENTILATED RING WING HYDROFOILS

I. Introduction

The present report describes a series of experiments on a family of simple conical ring wings in fully wetted and ventilating flow. The general characteristics of ring wings in uniform flow are well known. Ring wings have found application in marine propellers, aircraft, underwater bodies such as torpedoes, and depth bombs. The function and description of many of these applications are to be found in Reference 1. The general theoretical background of ring wings is dealt with in References 2 through 9. A typical and somewhat historical application of ring wings to a torpedo is given in Reference 10.

All of the foregoing references and applications are concerned with fully wetted flow. That is, the fluid is either all liquid or all air. Because of the proximity of a neighboring free surface in a flow of liquid or perhaps by the deliberate injection of gas into a liquid flow, a two-phase flow may take place. The cavity of gas so formed may occupy only a portion of the boundary of the body so affected, in which case it is called partly cavitating (or partly ventilating if a supply of air is the cause of the cavity), or the cavitating or ventilating region may entirely surround the body except near the nose. In this case the flow is called supercavitating or superventilating.* The object of the present work is to study and to treat experimentally some of the problems arising with superventilating and partly ventilating ring wings.

Interest in these problems is due to the fact that this subject has great intrinsic value and is a nearly unexplored field of practical

*The words "ventilating" and "cavitating" are often used interchangeably in the literature and although ventilating is to be preferred when the cavities are air-supported, both terms are often used to describe this type of flow.

and theoretical treatment. This interest is also stimulated by the possibility of devising new schemes of force control which might augment or replace altogether the conventional rudders found on ships or possibly such devices as torpedoes which commonly employ a ring tail. The possibility of such an application was originally suggested by K. Smith and was followed up in the work of Lang and Daybell (Reference 11), in which water tunnel tests were carried out at the California Institute of Technology on normally fully wetted two-dimensional hydrofoils. Air was injected at various points on the hydrofoil, and it was observed that the resulting forces on the hydrofoil were greatly altered.

Few experimental or theoretical results on ventilating or cavitating flow past ring wings seem to be available. The only theoretical work known to the authors is an analytical study carried out with the aid of the rheo-electric analogy on the axisymmetric cavitating flow past a ring wing (Reference 12). In this work, use is made of linearized free streamline theory in setting up the approximations of the analogy. Several interesting examples are given in which the ring cross-sectional profile consists of straight line segments. All of these examples, however, have the pressure surface of the ring wing on the outside of the ring; the cavity that is thereby formed thus lies on the inside of the ring rather than the outside. The flow within the ring is therefore accelerated - as in a Kort nozzle - and not retarded, as would be more typical of shrouded propeller and pump-jet practice. The results in Reference 12 are not therefore directly applicable to these configurations and, being the results of an analogy, are not readily capable of generalization.

With these factors in mind it was decided to study the ventilated flow past ring wings using primarily an experimental approach. In application, the ring wing would almost certainly be used in conjunction with another body - such as a propeller shaft or hub - or it may be near another object, such as the hull of a ship as is treated in Reference 7. It was decided to begin by studying

the isolated ring wing and to defer consideration of the complications introduced by the presence of other bodies in the flow field. In such an experiment a number of different kinds of forces occur that are of interest. These include overall forces, such as lift, drag and moment on the complete ring assembly which depend on the ring geometry, ventilation state, and upon the attitude of the ring to the oncoming flow. It is just these forces that one needs to know in order to estimate the effectiveness of the ring as a means of control. There are in addition other internal forces which arise from the varying distribution of pressure around the periphery of the ring, and from the leading edge to the trailing edge. These may be summed up into a radial force, the direction of which is parallel to a radius and which in general varies with polar angle around the ring. The unbalanced side force caused by an unequal distribution of the radial force around the periphery of the ring causes the lift force. There is in addition an axial force. The integrated component of this force gives the pressure contribution to the drag.

In the present experiments the external forces on four ring wings were investigated. The experimental rings all had a maximum diameter of six inches. The chords were 2, 3, 4 and 6 inches respectively. A cross-section view of the 3-inch chord ring wing is shown in Fig. 3. Complete lift, drag and moment data were taken for this family of ring wings for fully wetted flow as well as for various conditions of ventilating flow. These forces were measured, as will be discussed in the following section, by means of an external strain gage force balance. The 2-inch chord model is shown installed on the balance in the Free Surface Water Tunnel in Fig. 4. This arrangement made it possible to measure the overall lift, drag and pitching moment of the ring assembly. However, it was not possible by this means to measure the radial forces previously mentioned. For this purpose it is necessary to have detailed knowledge of the local forces around the periphery of the ring. It was for this purpose that a pressure distribution model was made. Other means may

be used to measure the radial force coefficient. However, it seemed best to proceed with a pressure distribution model as this would permit a more detailed analysis of the radial force coefficients than would otherwise have been possible. The pressure distribution model is mounted on a reflection plane. It is shown ventilating in Fig. 5. However, because these models are relatively more expensive than the complete ring assemblies, only one series of pressure distribution measurements were made; these were carried out on a ring of 3 inches chord. The diameter of the ring wing was the same as before, namely 6 inches.

The last series of experiments were concerned with the effects of incomplete, or partial, ventilation around the periphery of the ring. Fig. 6 shows a photograph of such a vented condition on a ring of 2 inches chord. It can be seen that the lower half of the ring is fully wetted, while the upper half is ventilated. As in the case of Figs. 4 and 5, the ventilation is from the leading edge. In Fig. 6 ventilation over the bottom half is prevented by sealing off the supply of ventilating air. To secure the abrupt termination of the ventilation seen in Fig. 6 it was necessary to install small fences which prevented the ventilation from occurring around the entire periphery. This was a consequence of the simple type of profile shape chosen, as will be discussed later.

II. Description of Apparatus and Experimental Technique

1. Facility Description - The experimental work described in this report was performed in the Hydrodynamics Laboratory at the California Institute of Technology. The Free Surface Water Tunnel was the experimental facility used. Reference 13 describes in some detail the facilities of the laboratory and in particular the operation of the Free Surface Water Tunnel.

In the first test series, the principal measurements made were those of the total forces acting on the complete ring assemblies. To accomplish this, the ring models were held by a strut which in turn

was supported by a force balance. This balance measured the forces and moments which acted on the models. The balance was rigidly attached to "ground" above the water surface and the support strut held the model submerged in the flow. The objective of the second series of tests was to determine the pressure acting at various points on the model. A complete series of such measurements would yield the total pressure distribution on the model. To accomplish this, a rigid metal plate was mounted at the plane of the water surface. The surface of this plate provided a plane of symmetry for the flow, and was hence called a "reflection" plane. In this way the Free Surface Water Tunnel was converted into a closed jet tunnel having a working section approximately 20 inches square. The model in this case consisted of a half ring mounted on the reflection plane. Figs. 7 and 8 are general views of the experimental setups for the two different tests.

Tunnel velocity was obtained by means of a mercury-biased, water manometer which measured the pressure from a total head tube located upstream in the tunnel nozzle. Cavity pressures were measured using a water manometer connected to a small hole drilled in the side of the model which communicated to the cavity. Air was bled slowly through the cavity pressure measuring lines to insure that they would be free from water. This air flow resulted in a small zero offset in the cavity pressure readings which was accounted for in the data reduction process. This zero shift was kept constant for each cavity pressure measurement by means of adjusting the air flow rate before each cavity pressure reading was made to an originally predetermined value for which the pressure drop due to this air flow was known. The main cavity air supply was measured using a Fisher-Porter flow meter and applying the proper corrections for line pressure and temperature. The forces were measured on the models by means of a Task Corporation six component electrical strain gage balance energized by Microdot DC power supplies. Each of the Task balance channels was displayed on a Non-Linear Systems digital

voltmeter. Wiancko pressure transducers were used as the readout system for the pressure distribution models, and the outputs of these pressure transducers were likewise monitored by the NLS voltmeter. Both the force and pressure measuring systems will be described in more detail later.

To determine the pressure coefficients from the measurements made with the pressure distribution model, a detailed description of the flow in the vicinity of the model was necessary. Both the boundary layer thickness and the flow direction at the reflection plane near the model mounting location were measured. The result of these surveys are presented in Figs. 11 and 12. The boundary layer in the vicinity of the model is approximately one-quarter of an inch thick, and the flow deviation over the intercepted radius of the model is approximately 0.7 degrees.

2. Model Description. Before deciding upon the final configuration of the ring model, it was thought advisable to perform a series of preliminary design experiments which would help decide questions of model size and geometry, both in the fully wetted and cavitating flow regimes. In addition, the proposed system for supplying air to the model in the cavitating case could be studied.

Several important considerations dictated the choice of model section:

(a) Because of the exploratory nature of these experiments, the model should be easy to fabricate so that various model sizes, aspect ratios, etc., may be readily studied.

(b) The model should be able to operate fully wetted and fully ventilated, as well as partially ventilated, without changing its geometric description, i.e., cone angle, camber, or aspect ratio.

(c) The results should be amenable to comparisons with theory and past experiments, both to those pertaining to ring wings and to two-dimensional airfoils.

For these reasons, a flat plate section 1/8" thick and having a blunt trailing edge and a rounded leading edge was considered. The

shape of the flat plate section, especially the leading edge and air supply slit details, were chosen on the basis of experiments performed on an inexpensive rectangular hydrofoil.

This hydrofoil had a chord of 2 inches and a span of 9 inches. It was suspended vertically in the Free Surface Water Tunnel from the reflection plane and fitted with an end plate at its free end to reduce the three-dimensional tip effect. Rotation could be imparted about the vertical axis to vary the angle of attack. The results of testing this model indicated that the proposed system of distributing cavity air would be satisfactory for all but the very highest cavity air requirements. Also, these tests indicated that a section angle of attack of approximately 6 degrees was necessary to initiate clean separation of the cavity from the leading edge of the section.

Subsequent ring wing models were then constructed using the information obtained from these preliminary measurements. The final test model was constructed in the form of a cone having a total included angle of 12 degrees, and a section profile consisting of the 1/8-inch flat plate with the rounded semi-circular nose. Air was supplied to the cavity by means of a small slit approximately 0.005 inches wide machined in the brass model on the suction side at the point of tangency between the cylindrical leading edge and the flat surface (Fig. 3). The slit was connected to a plenum chamber machined into the flat plate section. This plenum chamber was in turn connected through an o-ring seal at the model-strut intersection to tubes which ran up the inside of the strut and connected to the main laboratory air supply.

Because of the effect of cone angle, ventilation could be achieved at smaller angles than the 6 degrees required for the two-dimensional model.

3. Force Measurements. The forces acting on the ring models were measured using the Task Corporation electrical strain gage balance. A general overall view of the test setup for taking force measurements is shown in Fig. 7. The model-strut assembly is

attached to the force balance which is in turn supported by the angle changing mechanism. Rotation takes place about a center arranged to coincide with the centerline of the model. Since the balance rotates with the model, the forces are measured with respect to the model axes. These forces are subsequently referred to axes parallel to the undisturbed flow upstream.

Although the strain gage balance is capable of measuring six force components, only three were actually taken as data; the other three were only monitored to insure proper yaw alignment. The three primary data that were taken were the model chord force, X, the normal force, N (obtained by algebraically summing the outputs of the forward normal force, N_1, and the aft normal force, N_2), and the pitching moment, M (obtained by taking the algebraic difference between N_1 and N_2 and multiplying by the distance between them). Conventional lift, drag and pitching moment were obtained by applying geometric transformations. A stepping switch allowed the output of each of the strain gage elements to be monitored sequentially. The outputs of all six of the strain gage channels were monitored continuously by means of six microammeters which provided an analog display of the forces acting on each of the load cell elements. This unit was helpful in the initial ranging of the balance and to prevent overloads when conditions were being changed on the model during the course of the experimental runs.

The NLS digital voltmeter which was used to obtain the data measures the average input voltage over preselected time periods up to ten seconds long. Due to the tunnel turbulence and velocity fluctuations, it was found advisable to use the longest averaging period. Actually, three such readings were taken from each force element and the average of each of these three readings was reported as the data point. Since the total normal force was the sum of both N_1 and N_2, it was thought advisable to take these readings as nearly simultaneously as possible. Therefore each of the three readings of

N_1 and N_2 (giving a total of six readings) were taken alternately, thus interspersing the individual forward and aft normal force readings. After the normal forces had been obtained, three separate readings of the chord force were obtained and then the model was changed to a new test condition and the process repeated. Rather than record the velocity at each test point, the velocity was constantly monitored and adjusted to give the same average value over the entire series of the test run. During the time in which the force measurements were being taken the cavity pressure and cavity air flow rate were measured and recorded.

For the case of the cavitating models, the cavity air supply was determined for each configuration that would give a fully developed cavity over the entire range of angles of attack. The air supply rate was then readjusted to this constant value before each data point was taken. The cavity pressure was measured and the variation in cavitation number at constant air supply for each of the test conditions is shown in Fig. 19. For the cavitating pressure distribution series of tests, air supply was not measured but cavity pressure was taken as data. Here, two distinct values of cavitation number were obtained. One occurred when the cavity length was adjusted to approximately three body diameters, and the other occurred when the cavity was allowed to grow until it extended beyond the plate and opened to the atmosphere, through the free surface. In the former case the cavitation numbers obtained were on the order of $K = 0.10$ and in the latter case they were approximately $K = 0.01$.

The balance was enclosed by a stainless steel waterproofing shield which had tapped holes drilled into it at various locations along its length to provide alternate model mounting locations. These bolt locations also helped to locate accurately small brackets from which weights could be hung to perform daily balance calibrations. In-place balance calibration could be performed quite quickly and was repeated each day before testing was resumed to allow for any drift that may have occurred since the previous day's testing. In fact, the actual

drift that occurred was very small, being on the order of approximately 4 microvolts (which corresponded to .04 pounds). Fig. 1 shows in schematic form the equipment used to obtain the model force measurements.

Fig. 9 shows a force model attached to the support strut. Four different model configurations were actually tested. As previously mentioned, they had chord lengths of 2, 3, 4 and 6 inches. The basic ring diameter at the leading edge was six inches and the total included cone angle of all the configurations was 12 degrees. The different configurations were obtained by adding detachable trailing edge sections to a basic 2-inch chord model (Fig. 3).

To minimize any possible interference between the model supporting strut and the ring wing itself, it was necessary to keep the thickness of the strut at an absolute minimum consistent with the requirements of strength and the geometrical arrangement of the tubes which supplied the ring with ventilating air and measured the cavity pressure. The manufacture of such struts is often delicate and time-consuming. The present strut was made quickly enough, however, by an electroforming process in which nickel was deposited over a mandrel fashioned of a low melting point alloy. The mandrel which was subsequently melted out incorporated all the necessary tubes and mounting fixtures.

In order to compare the results of these force tests and experimental techniques with previous analytical studies that had been evolved for thin rings of zero camber, i.e., cylindrical rings, it was desired to carry out tests on a cylindrical ring. A cylindrical ring was constructed for this purpose which had a diameter of six inches and a chord of three inches.

4. Pressure Distribution Measurement. In order to obtain more detailed information about the local force coefficients on the ring wing both in cavitating and fully wetted flow, it was decided to construct a pressure distribution model which would measure the pressure at any desired location on both the pressure and suction surfaces of the

model. For the purpose of this series of tests, the reflection plane previously mentioned was installed at the water surface in the Free Surface Water Tunnel. The model projected through this reflection plane and the central axis of the ring coincided with the reflection plane. In this way actually only half of the model projected into the flow. The model was set in a mounting disk which in turn was itself placed in a large circular hole in the reflection plane. The bottom surface of the mounting disk was coincident with the bottom surface of the reflection plane. Fig. 14 shows the model attached to this mounting disk. The disk could be turned about a vertical axis and as a result the yaw angle of the model with respect to the oncoming flow could be changed. Due to the geometry of the reflection plate-model system, this was equivalent to varying the angle of attack of a complete ring. Fig. 13 shows the model and mounting disk set in the reflection plane and the handle for setting the yaw angle. A row of eleven pressure taps was drilled on both the pressure and suction surfaces of the model in a chordwise direction. These holes communicated to a corresponding number of 1/16-inch diameter brass tubes which were placed circumferentially in slots turned in the surface of the model. These tubes broke out of the surface of the model for subsequent attachment to lines leading to the pressure measuring transducers at a point approximately 150 degrees around the ring from the location of the pressure taps. The chordwise pressure distributions were obtained directly by measuring the pressures at each of the different tap locations and the variation of pressure as a function of polar angle (or "spanwise" variation) could be determined by rotating the model about its central axis in the mounting disk which was set in the reflection plane. The pressure taps could only be rotated from approximately zero to 120 degrees. The remainder of the spanwise pressure distribution, that is from 120 to 180 degrees polar angle, was obtained by assuming that the pressures at a given polar angle between 90° and 180° at a positive model angle of yaw were the same as the pressures at a symmetrical polar angle (using the $\theta = 90^{\circ}$ line as the line of

symmetry) between zero degrees and 90 degrees for a model angle of yaw of the same magnitude but of opposite sign. This method of obtaining data limited the number of yaw angles (in this case only the positive yaw angles could be used) for which a complete spanwise pressure distribution could be obtained. Fig. 2 shows the geometry of the pressure distribution model in schematic form.

Prior experiments performed on the complete ring used in the force measurements indicated that a fully ventilated condition could be maintained without using the leading edge slot but with the use of an auxiliary air supply, although injection of air through a leading edge slot was generally required to initiate ventilation. Because of the comparative complexity of the pressure tap model, the leading edge ventilation slot was omitted and ventilation was initiated by imparting large yaw angles to the model. Once started, the ventilation could be maintained through small air supply ports in the image plate located near the trailing edge of the ring even though the angle of yaw of the ring was subsequently reduced.

The pressures were measured alternately on the suction and pressure sides of the model in the fully wetted flow and on the pressure side only in fully ventilated flow by means of eleven Wiancko 0-5 psi differential pressure transducers. The differential pressures were measured with respect to atmosphere. The signal from each of the transducers could be displayed sequentially by means of an eleven-position stepping switch on the NLS digital voltmeter. Fig. 8 is a view of the test area showing the model mounted in the tunnel, the NLS voltmeter, and the power supply for energizing the transducers. Fig. 15 shows the Wiancko pressure transducers secured to the back of the tunnel total head manometer.

As in the force measurement runs, the tunnel velocity was constantly monitored and adjusted to a predetermined value over the course of a run. Likewise, cavity pressure was measured in a manner similar to that for the force runs through a hole drilled in the reflection plane which communicated to the cavity. Cavity air supply rate and

cavity length were not measured.

5. Tunnel Corrections. All of the data taken for the force measurements were corrected for strut tare forces. To accomplish this the model was connected to an image support system attached to the floor of the tunnel. The image strut could be rotated, in a fashion similar to that of the main support strut, so that the model angle of attack could be changed about the model center. For determining the tare forces acting on the strut, only the 3-inch model was used over the same angle of attack range obtained in the force runs and the model was run both fully wetted and ventilated. For the cavitating case, cavity air was supplied through the main support strut, except that the air to the leading edge slit on the ring model was supplied by a hole drilled through the image strut and connected to the laboratory air supply by means of poly-flow tubing connected to the image strut and trailing downstream in the flow to a point where it was brought out through the free surface. The strut tare forces were determined with the strut held in approximately the same position relative to the model as it would have been during a normal force run, except that a small gap (about .050 inches) was left between it and the model. Weight and buoyancy tare forces were also obtained as a function of angle of attack for all of the models by swinging the balance and support strut with the various models attached through the angle of attack range both in air and at operating depth in still water.

The tare forces were all obtained at the standard operating depth of 0.675 feet and at the standard operating tunnel speed of 18.56 feet per second. Tare force corrections applied to data taken at different speeds and depths were obtained by multiplying the measured tare forces by the square of the velocity ratio and the wetted area ratio for the two different tare conditions respectively.

Interference forces due to the presence of the support strut in the fully wetted case were determined by holding the model by the support strut in the normal way and noting the change in the forces as the model was brought near the image strut. The interference

corrections obtained in this manner were not applied to the original data, however, both because of the small values obtained and because of the questionable validity of applying interference data obtained with a model having a 3-inch chord to the other models tested in this series. Fig. 10 shows a tare run being made under cavitating flow conditions and at an angle of attack of zero degrees.

III. Discussion of Results

1. Overall Forces. The overall experimental results obtained are presented in Figs. 16 through 20. In order to compare the present experimental results with previous analytical and experimental work, some tests were performed using a cylindrical model having a 6-inch diameter and a 3-inch chord. These tests were also designed to isolate the effects of the tunnel velocity and the free surface in the absence of such complicating factors as model cone angle, flow separation, etc., and hence these tests were performed at three values of the velocity and two different submergences. It can be seen from Fig. 16 that the main effect of velocity (or more probably Froude number) is to cause a slight shift in the angle for zero lift (about 1/4 degree). Since the rings are relatively close to the free surface, it is possible that the proximity of the free surface may have an effect on the forces experienced by the ring. It was not possible to answer this question exhaustively due to the geometric limitations of the working section. However, tests made on the cylindrical ring at a somewhat reduced submergence (0.425 feet) show only minor changes in the model forces. The slope of the lift curve is reduced approximately 4 percent and the angle for zero lift is shifted by about 1/4 degree. On the basis of these findings the subsequent experiments, except where noted, were carried out at a standard tunnel speed of 18.56 ft/sec. and at a standard submergence of 0.675 feet or 1.22 ring diameters to the model centerline. Because of the effect of gravity on the free surface of the tunnel and on the cavity formed during the ventilation experiments, it can be expected that the Froude number

will be a significant modelling parameter. To vary the Froude number without encountering severe problems of either tunnel blockage or real fluid effects predominant at small Reynolds numbers, would require a much larger working section. It is interesting to note, however, that the standard model test conditions, i.e., 18.56 ft/sec. and 6-inch ring diameter, would correspond to a 21-inch diameter ring wing at a speed of 20.6 kts. This figure is not so low as to be uninteresting in applications, and from results presently to be discussed it indicates that the effects of gravity will, if anything, be less for prototype conditions than in the tunnel experiments.

Experimental results for the conical rings are shown in fully wetted flow in Fig. 17 and in fully ventilated flow in Fig. 18. The slopes of the lift curves are higher for the fully wetted results than for the ventilating, though not by much. It will be seen that the fully wetted cones had largely a separated flow - a condition resembling the ventilated flow itself. Fig. 20 shows the effect of Froude number (or tunnel velocity) on the aspect ratio two ring. The angle for zero lift is clearly Froude number dependent. Since the interior of the ventilated ring is filled with water and the outside of the ring is exposed to the constant pressure of the cavity, a major portion of the observed lift must be due to the weight of the enclosed liquid. The resultant force due to this liquid was reduced to coefficient form for each of the test velocities and subtracted from the observed lift coefficients. It can be seen that the resultant curves tend to coalesce. The data shown in Fig. 18 have been similarly corrected and presented in Fig. 21. The curves thus obtained do not show zero lift at zero angle of attack, and indeed this zero lift angle does not remain exactly constant for the various rings and tunnel velocities. This is to be expected since the photographs of the cavities show (Figs. 4 and 10) that due to gravity, the cavity has a pronounced vertical asymmetry, and that because of blockage of the flow by the cavity, the free surface of the tunnel becomes appreciably distorted. It is not yet possible experimentally to distinguish these two effects. Nevertheless, the weight of the

water contained within the ring is the major effect.

The results of the pressure distribution measurements which will be presently discussed are compared with the full ring measurements for the 3-inch (aspect ratio two) ring in Fig. 22. These results, on the whole, agree well though they are not identical. This is undoubtedly due to two different effects; the direction of gravity in respect to the definition of angle of attack is different in the two types of measurements. From Figs. 1 and 2, as well as the photographs of Figs. 4 and 5, it can be seen that nothing corresponding to the weight of the enclosed liquid could arise in the pressure distribution measurements. However, the two lift-slopes are different too. This can be explained again by the different orientation of the gravity force and also by the different conditions prevailing for tunnel interference for the reflection plane mountings. The pressure distributions alone do not enable one to determine frictional drag nor the leading edge drag in ventilation conditions (the latter because severe space limitations prohibit placing a sufficient number of pressure taps on the small leading edge). Flat plate friction drag estimates were made of the wetted portion of the ring at the appropriate Reynolds number and for the leading edge pressure drag, it was assumed that the drag was the same as on a circular cylinder the same diameter as the leading edge and with a length equal to the circumference of the ring. These estimates (Fig. 22) agree quite well with the measured drag force on the 3-inch ring.

The foregoing experiments all deal with a basically axisymmetric flow. Two experiments were carried out in which only a portion of the circumference of the ring was ventilated. The ventilating air itself was prevented from issuing from the nose slot by taping the leading edge, as can be seen in Fig. 6. However, because the basic wetted flow past these rings is separated - at least near the leading edge of the cone - the ventilation tended to migrate around the full extent of the circumference. This migration was prevented in these experiments by the attachment of fins or fences

aligned with the free stream direction and only large enough to span the cavity at the ring. The resultant cross force due to the partial ventilation is shown in Fig. 23 for the two- and three-inch rings. It can be seen that the magnitude of the force developed by the partial ventilation is equivalent to about an angle of attack of 12 degrees on the entire fully wetted ring. The resulting vertical force is directed downward for the ventilating condition shown in Fig. 6.

It should be remarked that had the basic ring foils not been separated near the leading edge, there would have been no necessity for the ventilation fences. The fences contribute a lift force opposite in direction to the developed cross force, so that the results of Fig. 23 are at least conservative.

The slopes of the lift coefficient curves at zero angle of attack are summarized in Fig. 24 for all of the rings tested. It can be seen that the fully wetted models of aspect ratios 1.5 and 2 approach fairly closely the performance of the ventilated rings, suggesting strongly that they are in fact separated flows resembling the ventilated flows except for having a different "cavity" pressure. The highest aspect ratio fully wetted conical ring approached Weissinger's theoretical values (Reference 3), and the cylindrical ring is very close to the theory. Visual observations on the aspect ratio three conical ring with small tracer bubbles of air showed that the separation bubble at the leading edge re-attached itself to the surface of the cone before the trailing edge, so that values of lift slope approaching the theoretical should in fact be observed.

The lift-slope values for the fully ventilating cases appear to approach the value of $\pi/4$ as the aspect ratio becomes large. It is easy to show that this limit is the correct one for a ring wing of infinitesimal chord and zero cavitation number and small cone angle. It is, in fact, precisely one-quarter of the lift slope for the fully wetted ring of infinite aspect ratio and, as is well known, for small angles of incidence to the flow a cavitating flat plate hydrofoil at zero cavitation number has one-quarter the lift of a fully wetted hydrofoil. This

"one-quarter rule" is surprisingly well followed for the complete rings even at the aspect ratios tested. The actual ratios of the ventilated lift slopes to those of the fully wetted theory of Weissinger are 0.28, 0.29 and 0.19 for the aspect ratios 3, 2 and 1.5 respectively. All of these vented flows have cavitation numbers somewhat higher than zero (Fig. 19) which can be expected to increase the lift slope somewhat.

2. Pressure Distributions. Pressure distributions on the aspect ratio two ring are shown in Figs. 25 to 27. They include fully wetted flows and two different cavitation numbers in the ventilated condition. Pressure distributions are shown for several polar angles θ around the ring as sketched in Fig. 2. It is quickly apparent that the fully wetted distributions exhibit large regions of separation - especially at the largest angle of attack.

Each of the pressure distribution curves was numerically integrated to give a local normal force coefficient as a function of the polar angle around the ring, and these were then plotted as a function of the polar angle as shown in Fig. 28. The effects of the tunnel swirl can clearly be seen in this figure by examination of the curves for the normal force coefficient at zero angle of attack. If there had been no swirl, these lines should be horizontal and independent of polar angle. The amount by which they deviate from a horizontal line drawn through their maximum point (which occurs at a polar angle of 90 degrees) indicates the effect of the swirl at each polar angle. The effect of the tunnel swirl on the normal force coefficients can be eliminated at all other angles of attack by adding to them this incremental difference at each polar angle. (This tacitly assumes a linear behavior of force coefficients with local flow angle.) This was done for one of the cavitating runs and a diagram of normal force coefficient versus polar angle which has been corrected for swirl at an angle of attack of 4 degrees and a cavitation number of 0.01 is shown in Fig. 29. This distribution is well fitted by a cosine curve. Velocity distributions were calculated from the pressure distributions, the effect of swirl

being treated as above. From these the distribution of bound circulation was calculated and is shown in Fig. 30. Within the accuracy of these calculations this curve is again adequately fitted by a cosine curve. Such a distribution gives rise to an upwash consistent with the ring acting as a minimum induced drag lifting surface (Reference 2).

A comparison can be made between the experimentally determined values of lift curve slope and those obtained in which only bound vortex distribution is taken into account. For this purpose we shall instead proceed backwards and calculate effective lift slope of the two-dimensional hydrofoil section which would be needed in a strip theory and compare the results so obtained to the corresponding isolated cavitating flat plate hydrofoil. It is easy to show that the radial inwash angle due to a sinusoidal polar distribution of bound vorticity Γ is $57.3\ \Gamma/2\ U_\infty c$ degrees. The variation in local angle of incidence between 0 and 90 degrees polar angle is thus $4 - 57.3\ \Gamma/2\ U_\infty c$ degrees which, using the numerical result of Fig. 30, is 2.997 degrees. The corresponding variation in normal force coefficient is obtained from Fig. 29 from which one may deduce that the appropriate value of $dC_L/d\alpha$ for a strip theory would be

$$dC_L/d\alpha = 0.055/(2.997)/(57.3) = 1.02 .$$

This value is much lower than the isolated value for a cavitating flat plate at zero angle of attack, viz., $\pi/2 = 1.57$. The observed value of lift slope on the complete ventilated ring from pressure distribution data (Fig. 24) is seen to be 0.3. This is only 22.5 percent of Weissinger's theory and it is only 19.8 percent of Ribner's lifting line theory. It is probably safe to conclude that as the measured lift slope of the pressure distribution ring is low, there would be therefore an equivalently low value for the effective $dC_L/d\alpha$ of the appropriate strip theory. Assuming that ventilation has the same effect in two dimensions as for a lifting line ring, the equivalent lift slope of a strip would be

$$0.198 \times 2\pi = 1.24$$

some 20 percent higher than that calculated from a downwash distribution arising from bound vorticity alone. Although these numbers are

somewhat speculative in view of the tunnel swirl involved, it strongly suggests that downwash effects arising from the asymmetric cavity should be accounted for in such flows. It is likely that "source" effects due to the presence of the cavity will be even more important for partial ventilation.

As mentioned in an earlier section, the axisymmetric cavity problem has yet to be solved for the present configuration. A related problem is the cavitating two-dimensional flow past a flat plate near the ground. The flows are similar except that the one is a plane flow and the other is axisymmetric. Values of $dC_L/d\alpha$ have been computed for the plane flow at zero cavitation number (Reference 14). The two-dimensional values give a value of this parameter of about 2.4. The corresponding values for zero angle of attack on the ring can be estimated from Fig. 28 by dividing the average normal force coefficient by the local angle of incidence of the ring, namely 6 degrees. This gives a value of $dC_L/d\alpha$ equal to 2.8, which is in quite reasonable agreement with the two-dimensional value.

3. Effectiveness of the Partially Ventilated Ring. The measurements of cross force or lift developed by the partial ventilation technique shown in Fig. 23 can be interpreted in terms of a restoring or control moment for a specific underwater body. For the purposes of comparison, the Mark 13 torpedo shape was chosen. The effective moment was taken to be the observed lift force with a lever arm equal to the distance between the leading edge of the ring and the center of gravity of the torpedo. The results of this calculation are compared in Fig. 31 with the pitching moment as obtained by conventional elevator controls (this data being obtained from Reference 15). It is clearly evident that the partial ventilation scheme produces extremely large control forces compared with conventional means. These forces, in the present experiment, are in fact much larger than necessary.

The amount of the side force generated depends upon the fully wetted normal force coefficient, the aspect ratio and the extent of ventilation. As yet no theory is available to predict this result with

any certainty. For a first rough approximation, one may use the local values of normal force coefficient read from Fig. 28 for the ventilated and fully wetted portions of the ring and neglect completely the influence of the upwash at these sections. The results of such an elementary calculation determined from the pressure distributions of the 3-inch ring are respectively 17 and 33 percent low, i.e., conservative, for the one-half and one-fourth partial ventilation conditions. Hardly better could be expected for such a simple approximation. From this, however, one would expect that the lift-force would be proportional to the fully wetted normal force coefficient and possibly also proportional to the extent of ventilation. No information is at present available on the effect of air flow rate or the lift force developed although it would be expected that results would be similar to that in Reference 11. The actual air flow requirement for ventilation of the aspect ratio two and three rings is somewhat larger than for plane hydrofoils; whether this amount is "large or small" depends entirely upon the gases available and, as the entrainment phenomenon is largely a volumetric one, upon the available mass flow at the ambient pressure level.

Acknowledgments

The authors would like to acknowledge the help of the laboratory staff and would especially like to mention the efforts of Messrs. L. Whitcanack, W. Wilson, C. Eastvedt in carrying out the experiments; Mrs. L. Gaard in reducing the data; and Mrs. P. Henderson for preparation of the report.

BIBLIOGRAPHY

1. Sacks, A. H., Burnell, J. A., "Ducted Propellers - a Critical Review of the State of the Art", Advanced Research Division of Hiller Aircraft Corporation. Report No. ARD-232, 26 June 1959.

2. Ribner, Herbert S., "The Ring Wing in Nonaxial Flow", J. Aero. Sci., Vol. 14, 1947, p. 529.

3. Weissinger, J., "Some Results from the Theory of the Ring Wing in Incompressible Flow", Trans. from Advances in Aeronautical Sciences, Proceedings of First International Congress in the Aeronautical Sciences, Madrid, 8-13 September 1958, Vol. 2, pp. 798-831.

4. Kriebel, A. R., Sacks, A. H., Nielsen, J. N., "Theoretical Investigation of Dynamic Stability Derivatives of Ducted Propellers", Vidya Technical Report No. 63-95, 9 January 1963.

5. Kriebel, A. R., "Theoretical Investigation of Static Coefficients, Stability Derivatives, and Interference for Ducted Propellers", Vidya Report No. 112, March 31, 1964.

6. Kriebel, A. R., "Theoretical Stability Derivatives for a Ducted Propeller", Vidya Interim Report, October 18, 1963.

7. Kriebel, A. R., "Interference between a Hull and a Stern-Mounted Ducted Propeller", Vidya Report No. 161, September 30, 1964.

8. Weissinger, J., "Ring Airfoil Theory, Problems of Interference and Boundary Layer", Institut für Angewandte Mathematik der Technischen Hochschule, Karlsruhe, Germany, January 1959.

9. Reynolds, Jack F., "Lifting Surface Theory Applied to Isolated Ring Wings at Angle of Attack", NAVWEPS Report 8401, NOTS TP 3322, November 1963.

10. Levy, J., Knapp, R. T., "Water Tunnel Tests of the MK 13-1, MK 13-2 and MK 13-2A Torpedoes with Shroud Ring Tails", California Institute of Technology, HML Report No. ND-15.1, November 24, 1943.

11. Lang, T. G., Daybell, D. A., "Water Tunnel Tests of Three Vented Hydrofoils in Two-Dimensional Flow", J. of Ship Research, Vol. 5, No. 3, December 1961.

12. Luu, T. S., "Analytical Study and Rheoelective Simulation of Supercavitating Flows around Two and Three-Dimensional Hydrofoils", B.A.R.A. (47 Avenue Victor-Cresson, Issy-les-Moulineaux), December 1961.

13. Knapp, R. T., Levy, J., O'Neill, J. P. and Brown, F. B., "The Hydrodynamics Laboratory at the California Institute of Technology", Trans. A.S.M.E., Vol. 70, No. 5, July 1948, pp. 437-457.

14. Ai, D. K., Acosta, A. J., Harrison, Z. L., "Linearized Theory of a Two-Dimensional Planing Flat Plate in a Channel of Finite Depth - I", Hydrodynamics Laboratory, California Institute of Technology, Report No. E-110.2, April 1964.

15. Grady, R. J., "Hydrodynamic Coefficients of Torpedoes, Part I", NAVORD Report No. 544, 16 November 1953.

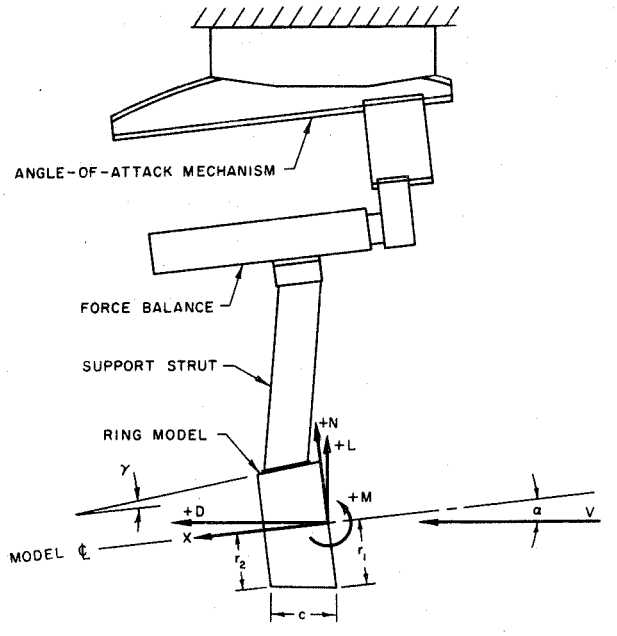

Fig. 1 - Forces on ring wing showing sign convention and the force measuring apparatus.

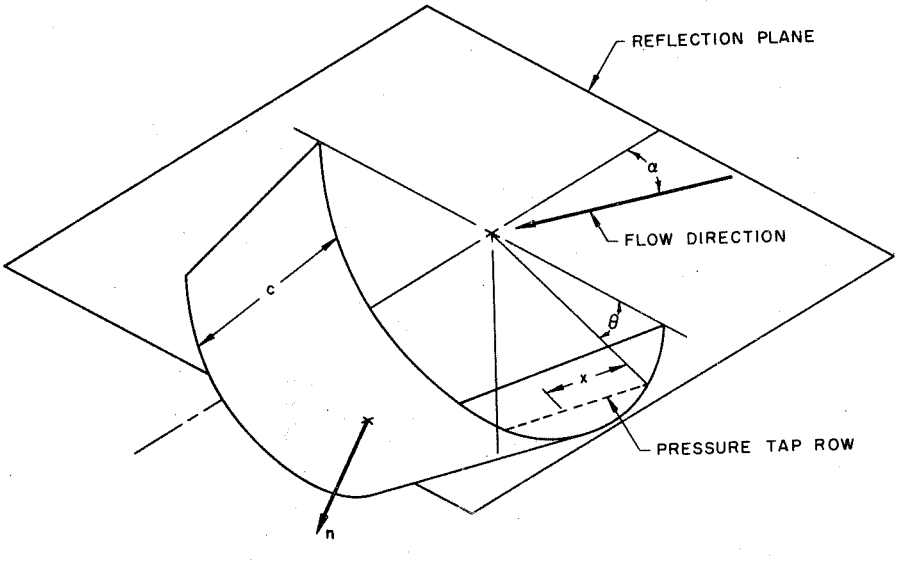

Fig. 2 - Pressure distribution model schematic, defining the pertinent parameters and sign conventions.

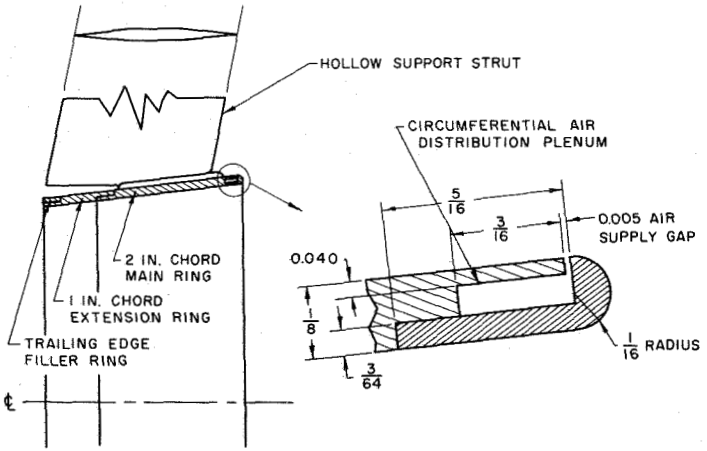

Fig. 3 - Sketch showing assembly ring wings and the ventilation slot at the leading edge.

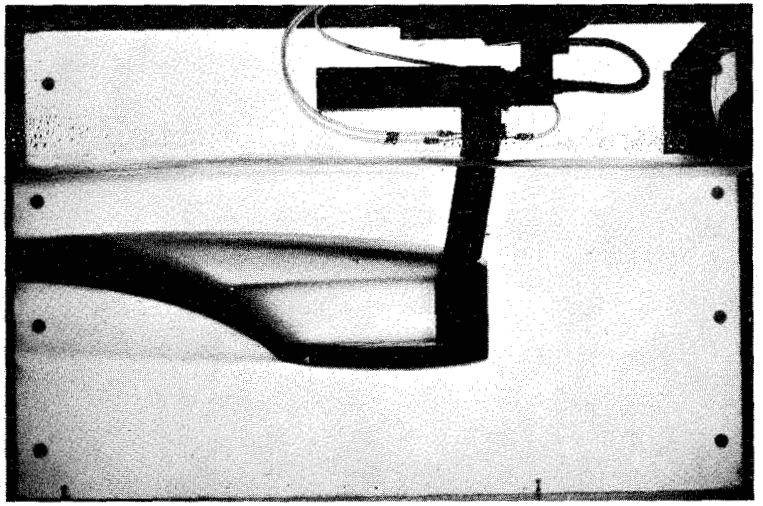

Fig. 4 - Fully ventilated ring wing. The chord is 3 inches and the diameter is 6 inches. The cavitation number is 0.13 and the angle of attack is zero degrees.

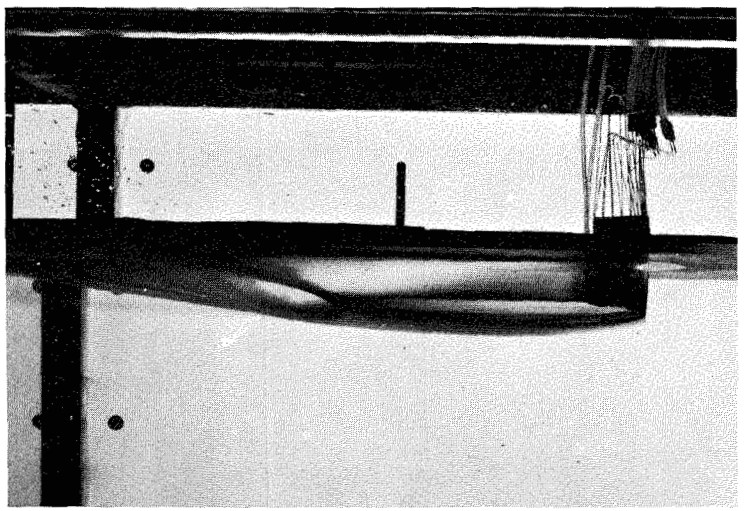

Fig. 5 - Reflection plane mounted pressure distribution model. Chord, 3 inches, k = 0.10, angle of yaw, 4^{o}. Flow velocity, 18.6 ft/sec.

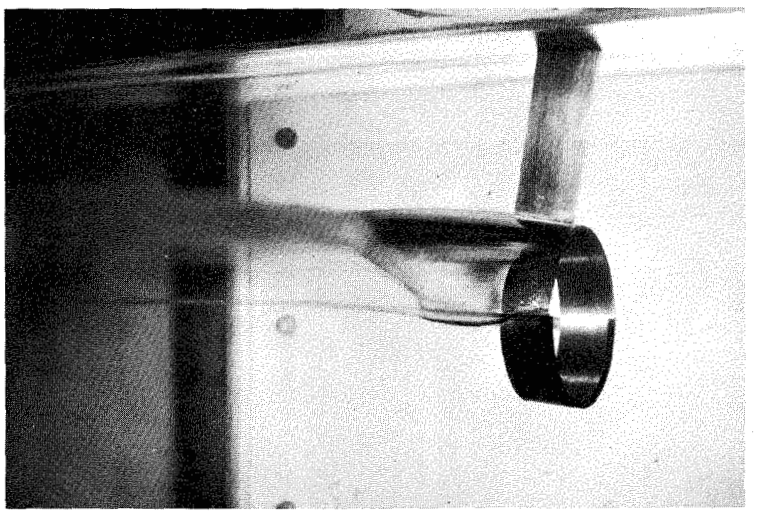

Fig. 6 - Partial ventilation over one-half the periphery of the ring for the 2-inch chord. (To prevent ventilation around the entire ring, small auxiliary "fences" are used.)

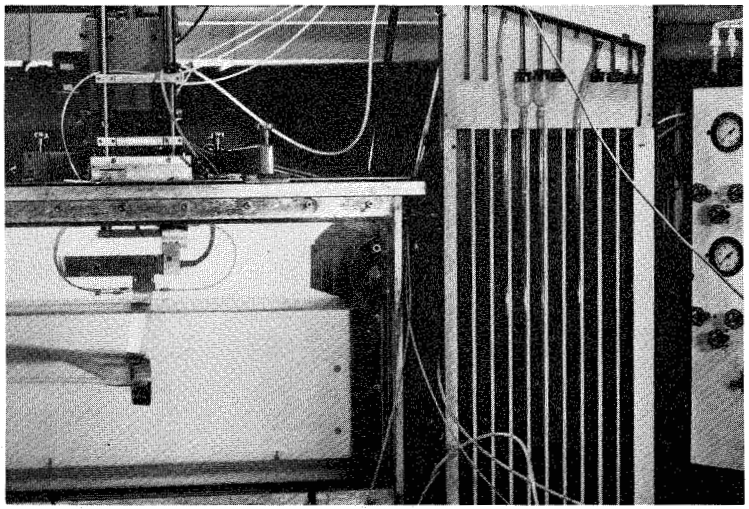

Fig. 7 - View of experimental test area for the determination of the forces acting on the models. The 2-inch chord model is shown installed in the tunnel working section, attached to the force balance.

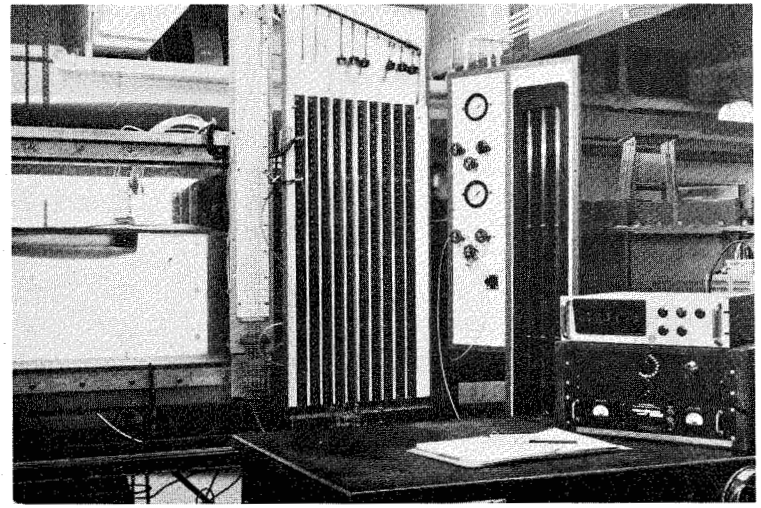

Fig. 8 - View of experimental test area for the determination of model pressure distributions.

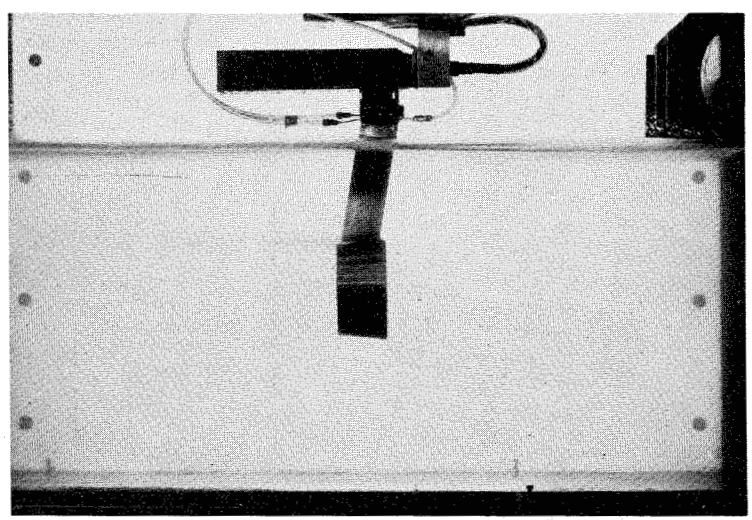

Fig. 9 - View of 3-inch force model attached to the support strut in the tunnel working section. The strain gage balance and air supply lines are also shown.

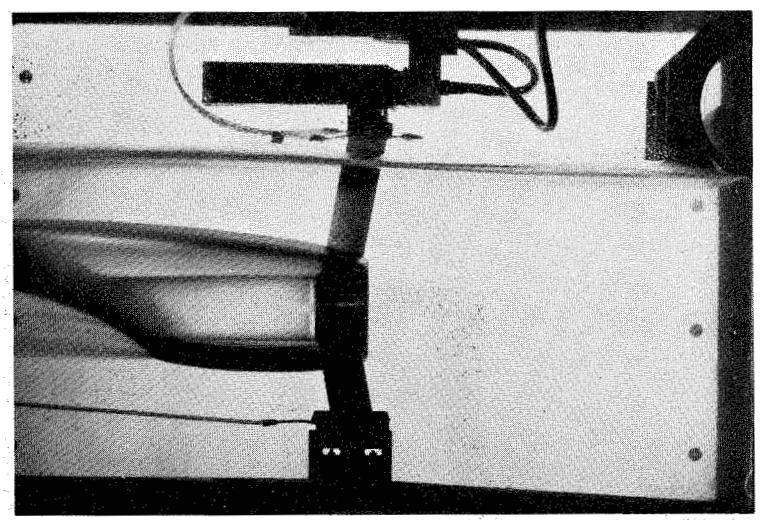

Fig. 10 - Model shown attached to image support strut for the determination of model tare forces.

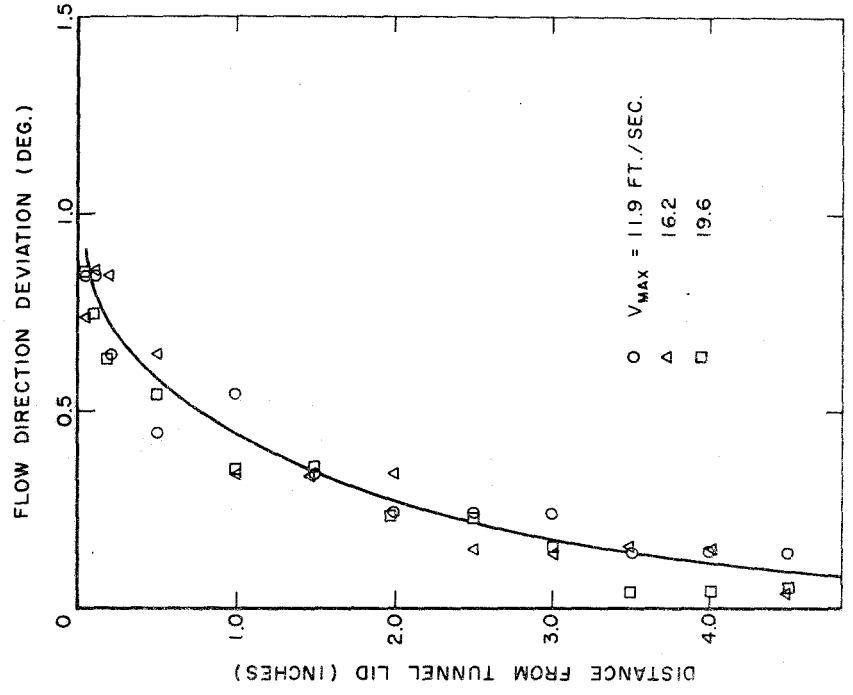

Fig. 12 - Flow direction as a function of depth from the reflection plane at the model mounting location. (Swirl is counterclockwise, looking downstream.)

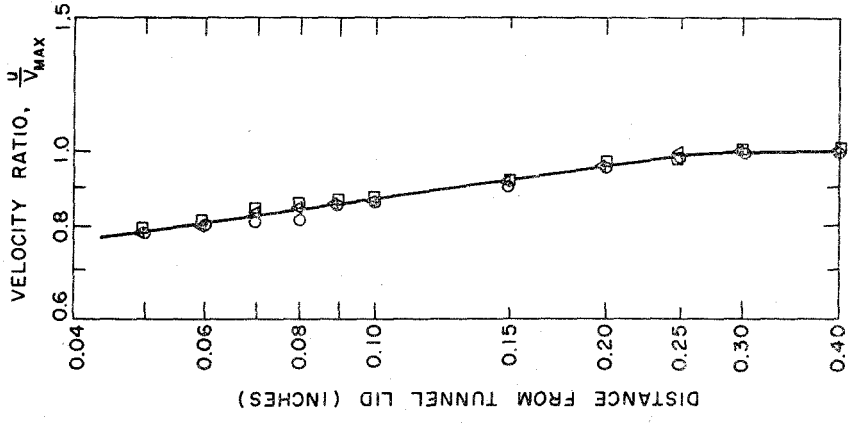

Fig. 11 - Velocity profile on the reflection plane at the model mounting location. (See Fig. 12 for a definition of symbols.)

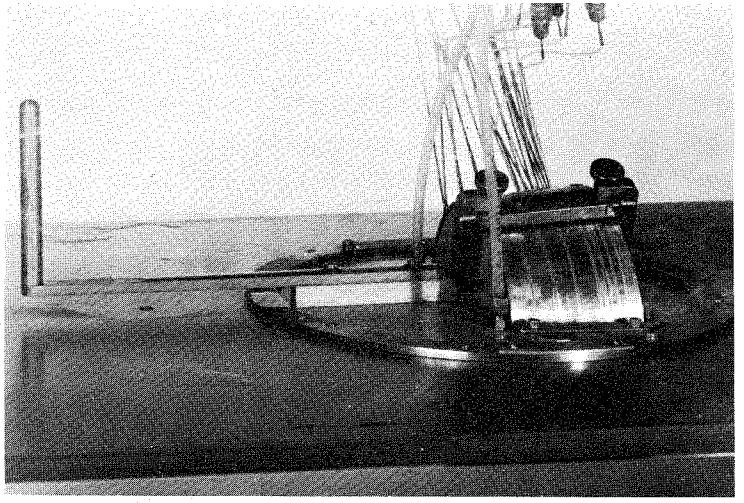

Fig. 13 - Pressure distribution model mounted in tunnel reflection plane.

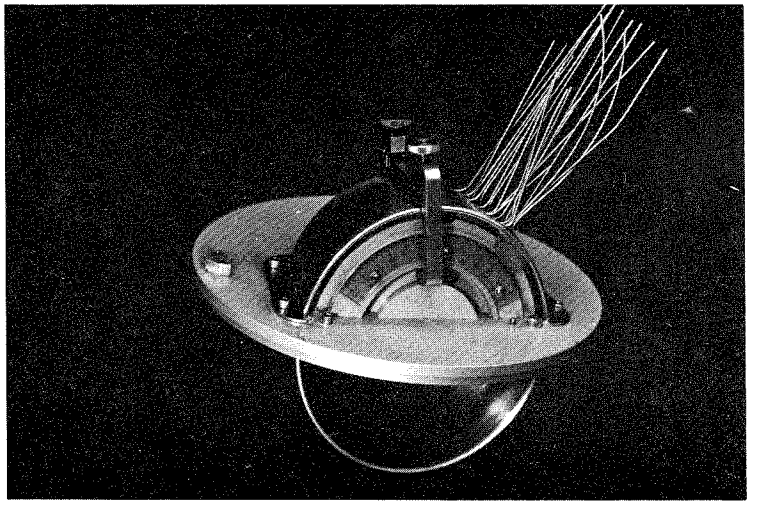

Fig. 14 - Attachment of pressure distribution model to mounting disk.

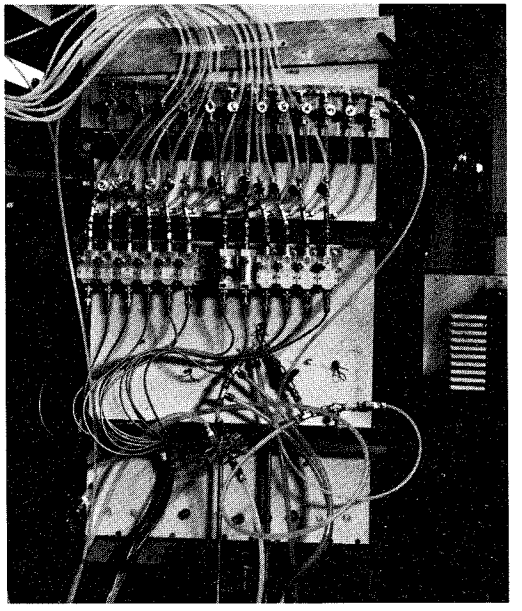

Fig. 15 - Wianko pressure transducers for pressure distribution measurement attached to back of tunnel total head manometer board.

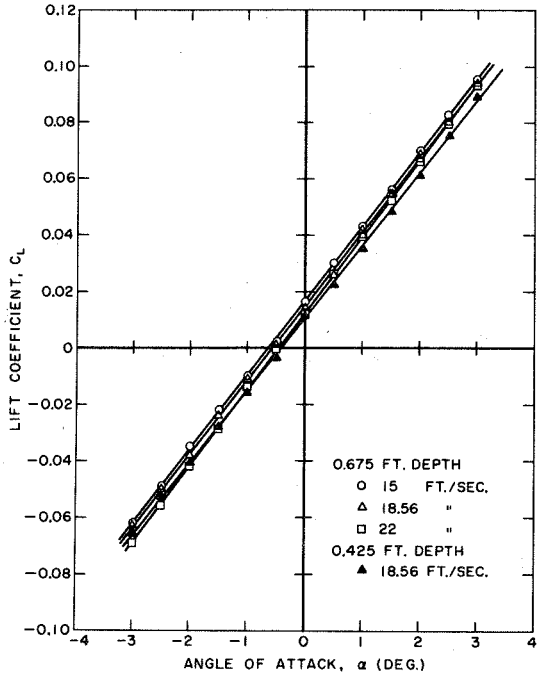

Fig. 16 - The effect of velocity and submergence on the lift coefficient of a 6-inch diameter cylindrical ring wing with 2-inch chord.

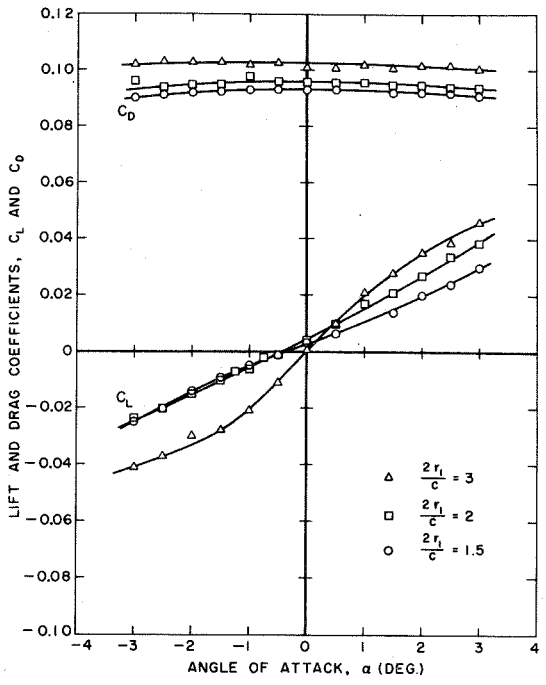

Fig. 17 - The effect of aspect ratio on the lift and drag coefficients of a fully wetted ring wing with a 12° included cone angle. The velocity is 18.5 ft/sec.

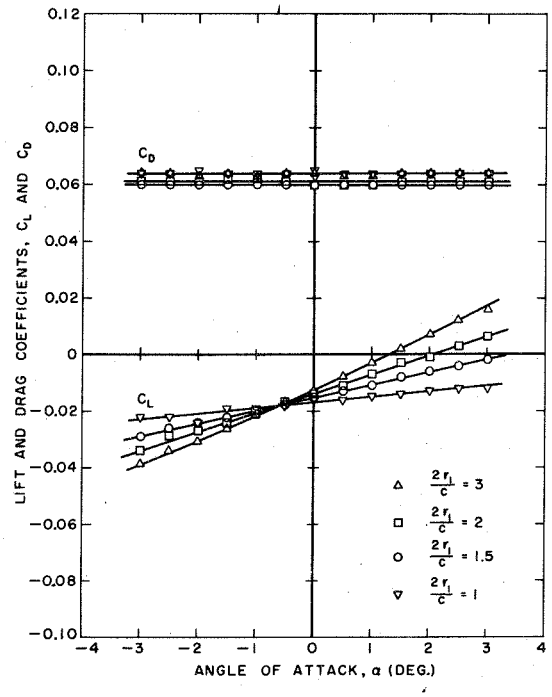

Fig. 18 - The effect of aspect ratio on the lift and drag coefficients of a fully ventilated ring wing with a 12° included cone angle. The velocity is 18.5 ft/sec.

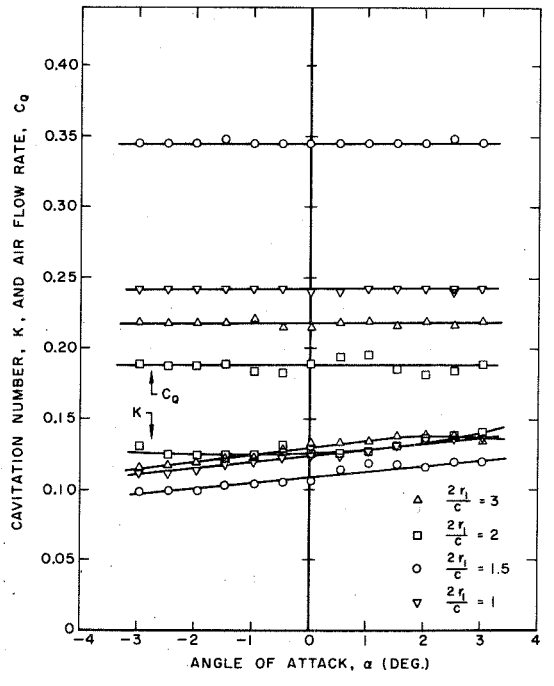

Fig. 19 - Variation of measured cavitation (ventilation) number at fixed air supply rates for conical ring wings at varying aspect ratios.

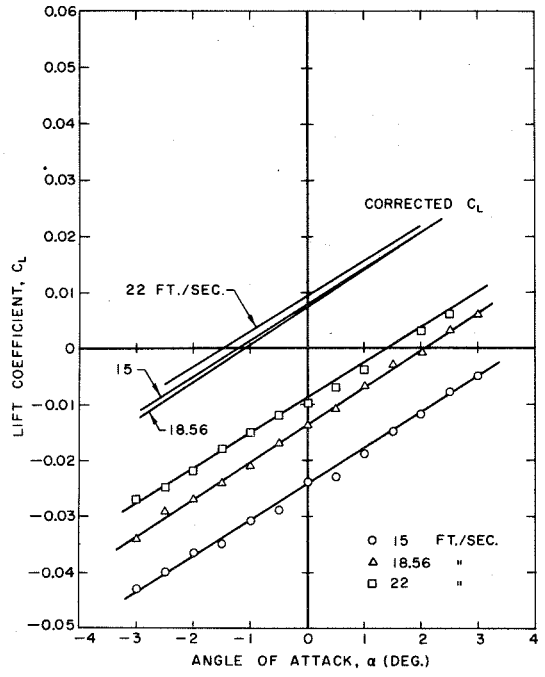

Fig. 20 - Lift coefficient versus angle of attack for the 3-inch cone at various tunnel velocities or Froude numbers in fully ventilated flow. (The lines labeled "corrected C_L" are the same as each of the experimental curves except that the weight of the water contained by the wing has been subtracted from the lift force.)

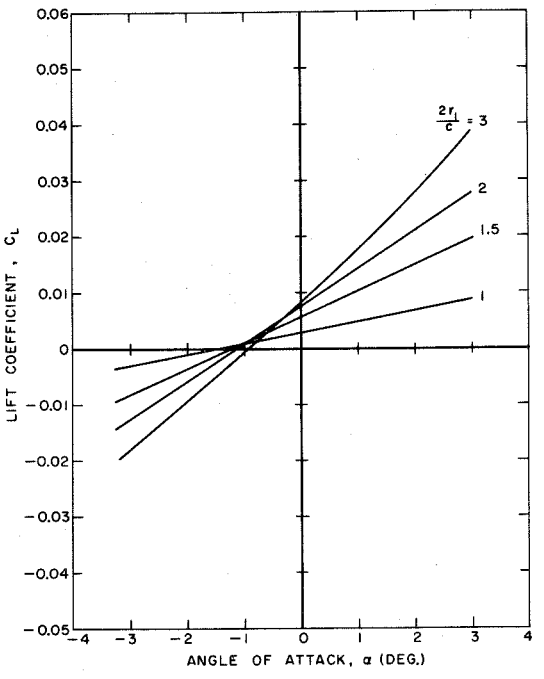

Fig. 21 - Lift coefficient versus angle of attack for the family of cones in fully ventilated flow corrected for the weight of water contained within the volume of the ring. Tunnel velocity is 18.56 ft/sec.

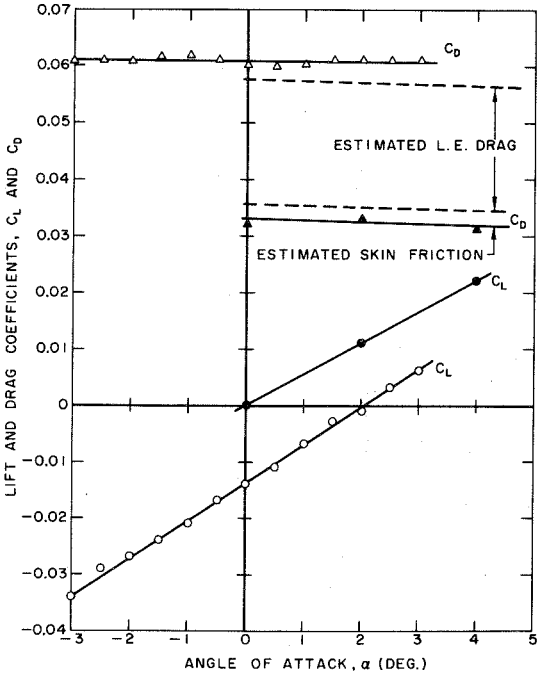

Fig. 22 - Comparison of 3-inch chord, fully ventilated ring with results of the pressure distribution model. The solid points are the result of calculations made from measured surface pressures on the model.

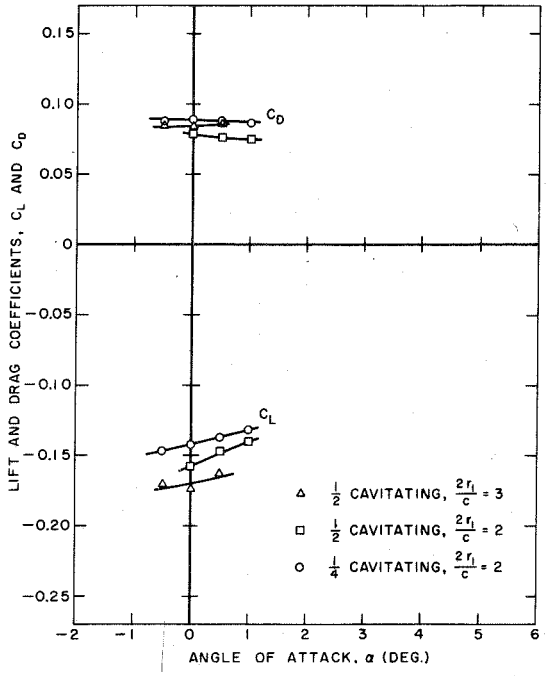

Fig. 23 - The effect of ventilating part of the ring circumference on the forces in the vertical plane for ring wings of several aspect ratios.

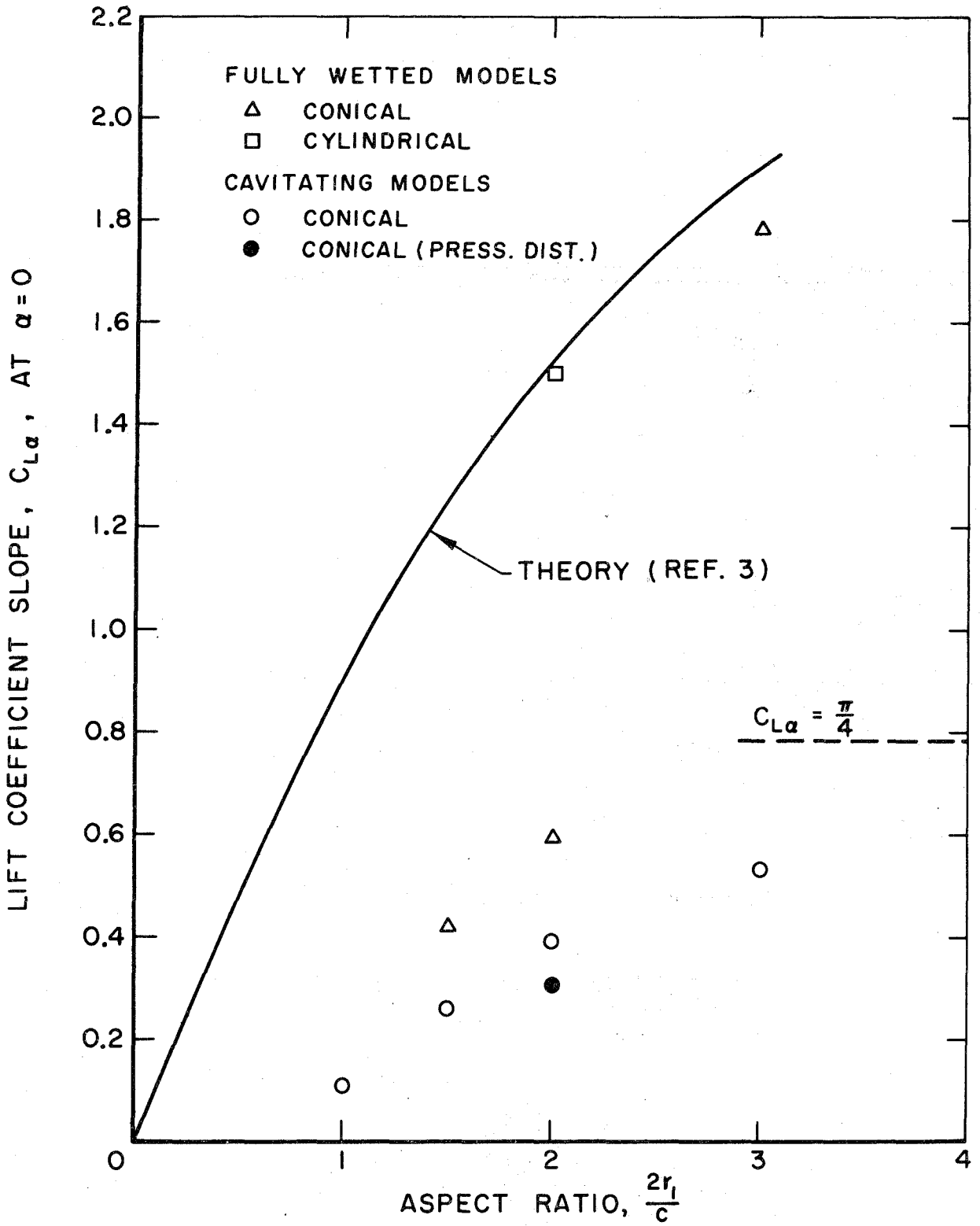

Fig. 24 - Lift slope values for the measured ring wings in fully wetted and ventilated flow. (Data was obtained with both the force models and the pressure distribution model.) Velocity is 18.56 ft/sec.

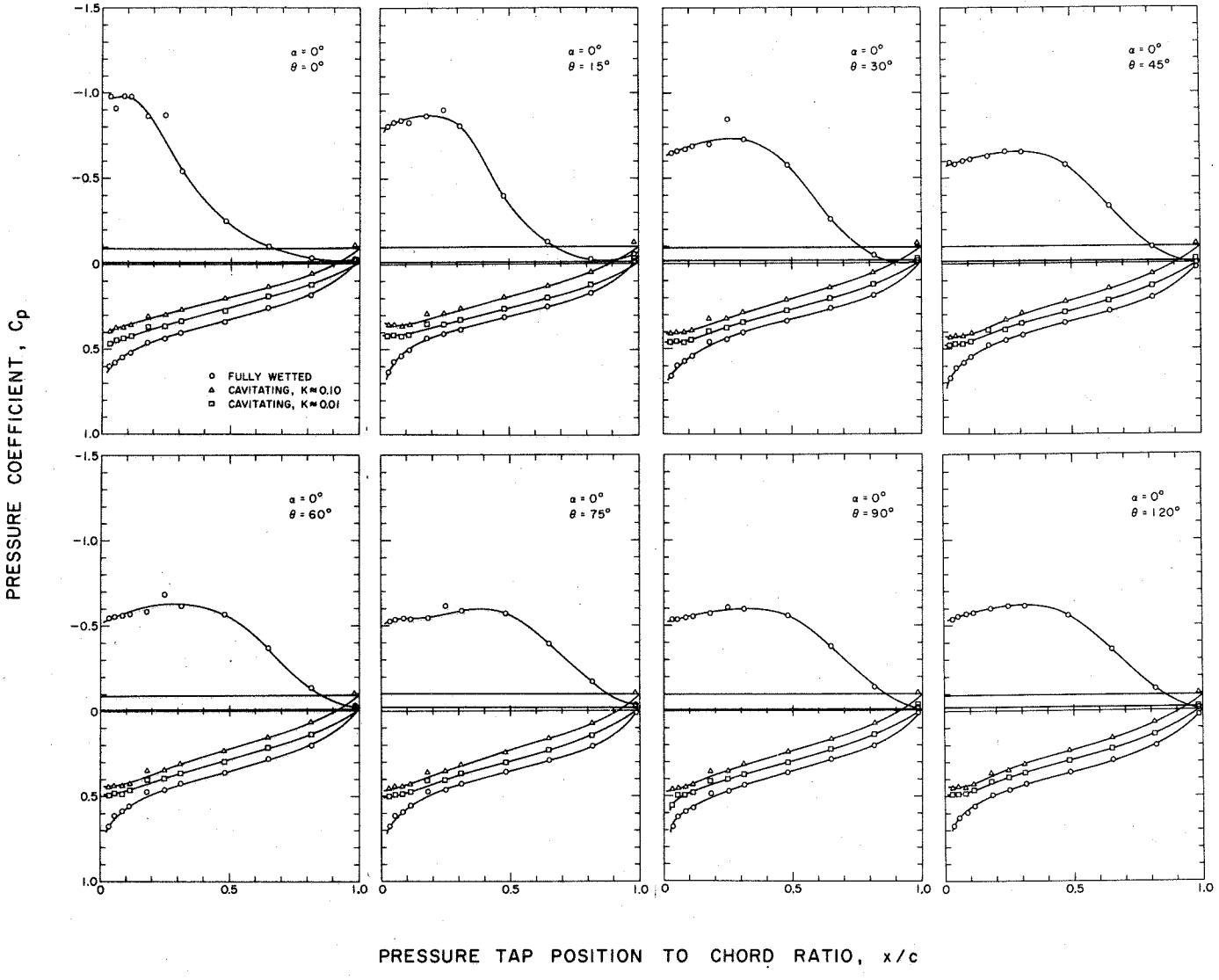

Fig. 25 - Pressure Distributions at Various Polar Angles around a Conical Ring of Aspect Ratio Two for Fully Wetted Flow and Ventilated Flow at Two Cavitation Numbers. Angle of Attack is Zero Degrees.

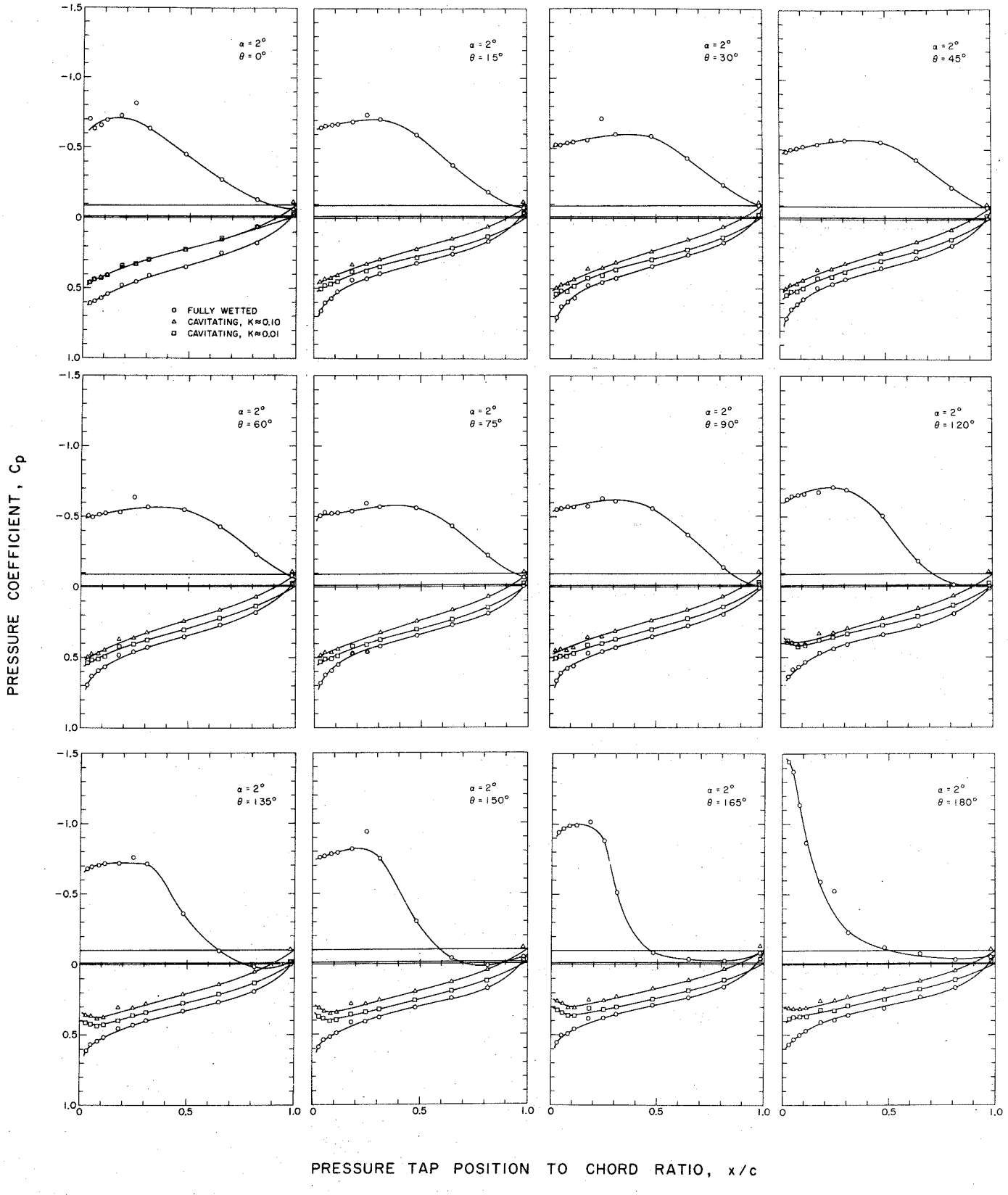

Fig. 26 - Pressure Distributions at Various Polar Angles around a Conical Ring of Aspect Ratio Two for Fully Wetted Flow and Ventilated Flow at Two Cavitation Numbers. Angle of Attack is Two Degrees. (Experimental points at polar angles greater than $\theta = 120^{\circ}$ were obtained at negative angle of attack.)

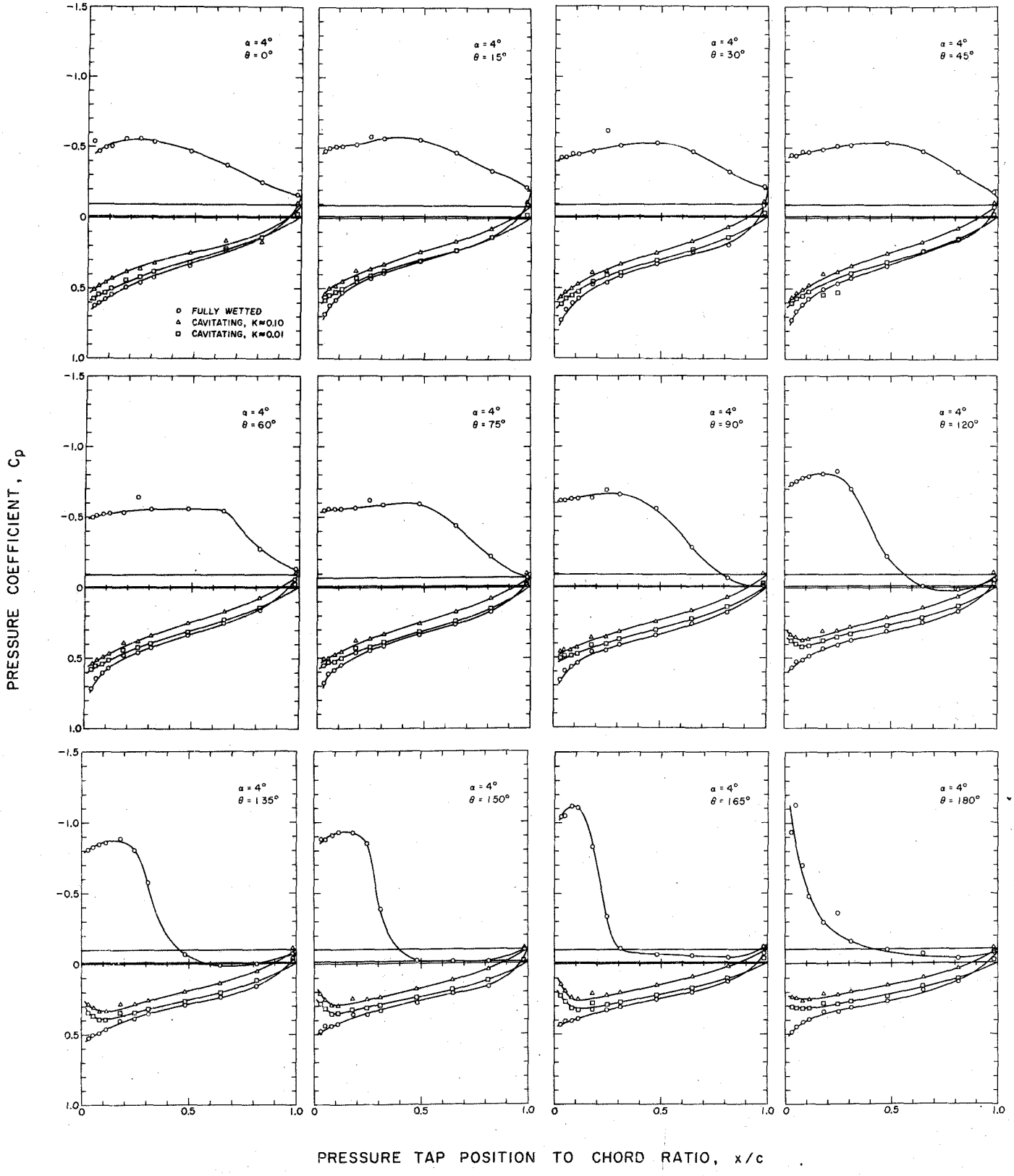

Fig. 27 - Pressure Distributions at Various Polar Angles around a Conical Ring of Aspect Ratio Two for Fully Wetted Flow and Ventilated Flow at Two Cavitation Numbers. Angle of Attack is Four Degrees. (Experimental points at polar angles greater than $\theta = 120^{\circ}$ were obtained at negative angle of attack.)

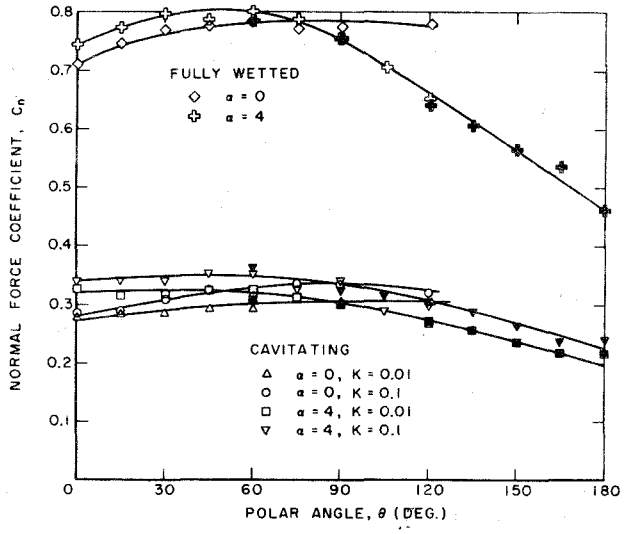

Fig. 28 - Radial force coefficients as a function of polar angle around a conical ring wing for fully wetted flow and ventilated flow for two angles of attack. The diameter-chord ratio is 2.0 and the half angle of the cone is 6 degrees. The solid symbols represent data obtained at negative angles of attack.

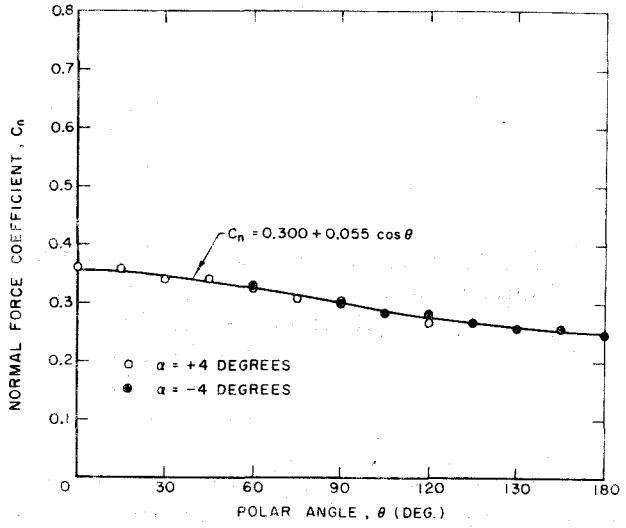

Fig. 29 - Normal force coefficient versus polar angle for a ventilated ring wing of 2.0 diameter-chord ratio corrected for effects of tunnel swirl. The cavitation number is 0.01 and the angle of attack is 4 degrees.

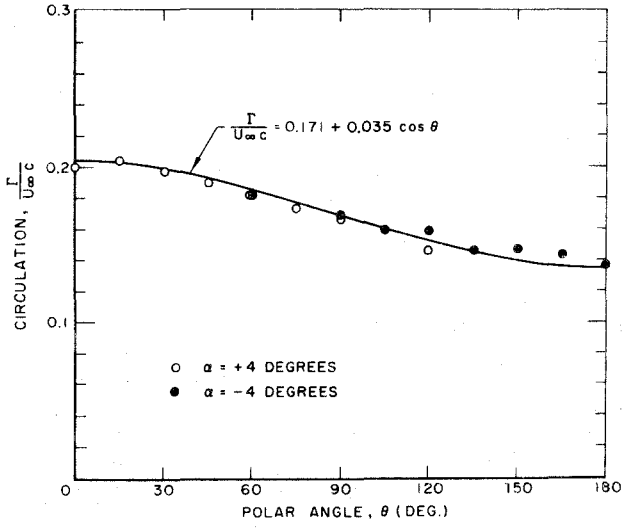

Fig. 30 - Distribution of circulation around the ventilated ring wing of Fig. 29.

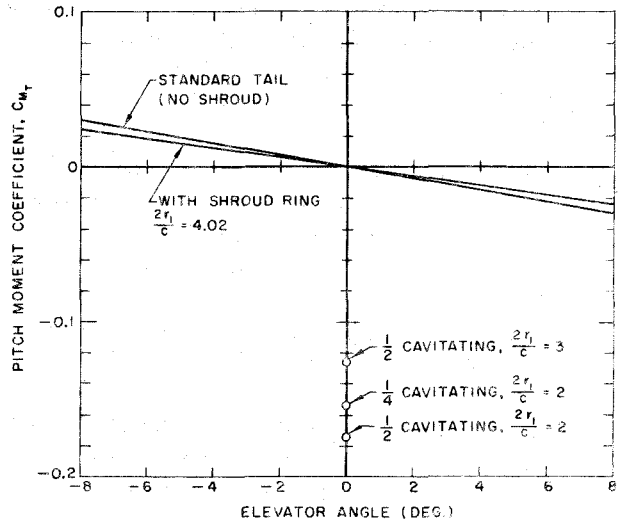

Fig. 31 - Comparison of the pitching moment that would be obtained by partial shroud ring ventilation with conventional elevator controls on the Mk 13 torpedo. The angle of attack of the torpedo is zero; the pitching moment is measured with respect to the center of gravity of the body.

DISTRIBUTION LIST

Agency	Copies
Chief, Bureau of Naval Weapons Department of the Navy, Washington, D.C. 20360	
Attn: Code RRRE-4	2
Code RUTO-32	1
Code RAAD-3	1
Code DLI-3	2
Commanding Officer and Director David Taylor Model Basin, Carderock, Maryland	
Attn: Code 601	1
Code 526	1
Commander, Naval Missile Center, Point Mugu, California	
Attn: Technical Library	1
Commander, Naval Ordnance Test Station Inyokern, China Lake, California	
Attn: Technical Library	1
Commander, Naval Ordnance Test Station Pasadena Annex, Pasadena, California	
Attn: Code P80	1
Code P5006	1
Commander, Naval Ordnance Laboratory White Oak, Silver Spring, Maryland	
Attn: Code 591	1
Code 750	1
Commanding Officer, Naval Underwater Ordnance Station Newport, Rhode Island	1
Officer in Charge, Naval Aircraft Torpedo Unit U. S. Naval Air Station, Quonset Point, Rhode Island	
Attn: R. Crowell	1
Commanding Officer and Director Naval Electronics Laboratory, San Diego 52, California	1
Commanding Officer, Naval Torpedo Station, Keyport, Wash.	
Attn: J. Mason	1
Commander, Naval Weapons Laboratory, Dahgren, Va.	
Attn: Technical Library	1

DISTRIBUTION LIST (continued)

Chief of Naval Research, Department of the Navy
Washington, D. C. 20360
Attn: Code 438 1
Code 466 1

Chief, Bureau of Ships, Department of the Navy
Washington, D. C. 20360
Attn: Code 421 1

U.S. Naval Academy, Annapolis, Maryland, Attn: Library 1

U. S. Naval Research Laboratory, Washington, D.C. 20390
Attn: Library 1

U. S. Naval Underwater Sound Laboratory
Fort Trumbull, New London, Connecticut
Attn: Library 1

Superintendent, U. S. Naval Postgraduate School
Monterey, California
Attn: Library 1

Air Force Office of Scientific Research (SREM)
Washington, D.C. 20333 1

National Aeronautics and Space Administration
Washington, D. C. 20546 3

Commander, Defense Documentation Center
Cameron Station, Alexandria, Virginia 22314 15

National Science Foundation, Washington, D.C. 20550 1

National Bureau of Standards, Fluid Mechanics Section
Washington, D. C.
Attn: Dr. G. B. Schubauer 1

Director, Applied Physics Laboratory, The Johns
Hopkins University, Silver Spring, Maryland
Attn: Library 1

Alden Hydraulic Laboratory
Worcester Polytechnic Institute, Worcester 9, Mass.
Attn: L. J. Hooper 1

Davidson Laboratory
Stevens Institute of Technology, Hoboken, New Jersey
Attn: A. Suarez 1

DISTRIBUTION LIST (continued)

Ordnance Research Laboratory
Pennsylvania State University, State College, Pennsylvania
Attn: G. F. Wislicenus 1

Hydrodynamics Laboratory, Department of Naval
Architecture and Marine Engineering,
Massachusetts Institute of Technology, Cambridge 39, Mass.
Attn: Library 1

Advanced Systems Engineering
Westinghouse Electric Corporation, Sunnyvale, California
Attn: M. S. Macovsky 1

Aerojet General Corporation, Azusa, California
Attn: C. A. Gongwer 1

American Machine and Foundry Company
P. O. Box 187, Station F, Buffalo 12, New York
Attn: G. F. Hussey 1

Clevite Ordnance, Division of Clevite Corporation
540 E. 105th Street, Cleveland 8, Ohio
Attn: T. Lynch 1

Eastern Research Group, 120 Wall Street, New York 5, N.Y. 1

Goodyear Aircraft Corporation, Akron 15, Ohio
Attn: R. R. Fisher 1

Grumman Aircraft Engineering Corporation
Bethpage, Long Island, New York
Attn: Research Department 1

Hydronautics, Inc., Laurel, Maryland
Attn: P. Eisenberg 1

United Aircraft Corporation Research Laboratories
East Hartford 8, Connecticut
Attn: F. S. Owen 1

Underwater Launch Department
Lockheed Missile and Space Division, Sunnyvale, Calif.
Attn: R. W. Kermeen 1

Hydrodynamics Laboratory GD/Convair
San Diego 12, California
Attn: R. H. Oversmith 1

DISTRIBUTION LIST (continued)

Therm Advanced Research Division, Therm, Inc.
Ithaca, New York
Attn: A. Ritter 1

Vidya Division, Itek Corporation
1450 Page Mill Road, Palo Alto, California
Attn: J. N. Nielsen 1

Unclassified

Security Classification

DOCUMENT CONTROL DATA - R&D

(Security classification of title, body of abstract and indexing annotation must be entered when the overall report is classified)

1. ORIGINATING ACTIVITY (Corporate author) Hydrodynamics Laboratory California Institute of Technology Pasadena, California	2a. REPORT SECURITY CLASSIFICATION Unclassified 2b GROUP

3. REPORT TITLE

Measurements on Fully Wetted and Ventilated Ring Wing Hydrofoils

4. DESCRIPTIVE NOTES (Type of report and inclusive dates)

5. AUTHOR(S) (Last name, first name, initial)

Acosta, Allan J., Bate, Jr., E.R., and Kiceniuk, Taras

6. REPORT DATE	7a. TOTAL NO. OF PAGES	7b. NO. OF REFS
June 1965	44	15

8a. CONTRACT OR GRANT NO. Nonr 220(54) - 61212 b. PROJECT NO. c. d.	9a. ORIGINATOR'S REPORT NUMBER(S) E-138.1 9b. OTHER REPORT NO(S) (Any other numbers that may be assigned this report)

10. AVAILABILITY/LIMITATION NOTICES

Qualified requesters may obtain copies of this report from DDC

11. SUPPLEMENTARY NOTES	12. SPONSORING MILITARY ACTIVITY
	Department of the Navy, Bureau of Naval Weapons, Fluid Mechanics and Flight Dynamics Branch

13. ABSTRACT

Force measurements and visual observations were made in a water tunnel on fully wetted and ventilated flows past a family of conical ring wings having a flat plate section geometry. The diameter-chord ratio was varied from one to three, and the total included cone angle was 12 degrees. The fully wetted flows all exhibited separation from the leading edge except for the largest diameter-chord ratio, a result which was in agreement with previous work. The effect of ventilation is to reduce markedly the lift curve slope. Pressure distribution measurements were also made under ventilating conditions for one member of this series. The effect of ventilation over only a portion of the circumference of the ring was also briefly investigated. Large cross forces were developed by such ventilation and some comparisons are made between this method of obtaining control forces and more conventional methods.

DD FORM 1 JAN 64 1473

Unclassified

Security Classification

14. KEY WORDS	LINK A		LINK B		LINK C	
	ROLE	WT	ROLE	WT	ROLE	WT
Ring Wing Ventilation Control Surfaces						

INSTRUCTIONS

1. ORIGINATING ACTIVITY: Enter the name and address of the contractor, subcontractor, grantee, Department of Defense activity or other organization *(corporate author)* issuing the report.

2a. REPORT SECURITY CLASSIFICATION: Enter the overall security classification of the report. Indicate whether "Restricted Data" is included. Marking is to be in accordance with appropriate security regulations.

2b. GROUP: Automatic downgrading is specified in DoD Directive 5200.10 and Armed Forces Industrial Manual. Enter the group number. Also, when applicable, show that optional markings have been used for Group 3 and Group 4 as authorized.

3. REPORT TITLE: Enter the complete report title in all capital letters. Titles in all cases should be unclassified. If a meaningful title cannot be selected without classification, show title classification in all capitals in parenthesis immediately following the title.

4. DESCRIPTIVE NOTES: If appropriate, enter the type of report, e.g., interim, progress, summary, annual, or final. Give the inclusive dates when a specific reporting period is covered.

5. AUTHOR(S): Enter the name(s) of author(s) as shown on or in the report. Enter last name, first name, middle initial. If military, show rank and branch of service. The name of the principal author is an absolute minimum requirement.

6. REPORT DATE: Enter the date of the report as day, month, year; or month, year. If more than one date appears on the report, use date of publication.

7a. TOTAL NUMBER OF PAGES: The total page count should follow normal pagination procedures, i.e., enter the number of pages containing information.

7b. NUMBER OF REFERENCES: Enter the total number of references cited in the report.

8a. CONTRACT OR GRANT NUMBER: If appropriate, enter the applicable number of the contract or grant under which the report was written.

8b, 8c, & 8d. PROJECT NUMBER: Enter the appropriate military department identification, such as project number, subproject number, system numbers, task number, etc.

9a. ORIGINATOR'S REPORT NUMBER(S): Enter the official report number by which the document will be identified and controlled by the originating activity. This number must be unique to this report.

9b. OTHER REPORT NUMBER(S): If the report has been assigned any other report numbers *(either by the originator or by the sponsor)*, also enter this number(s).

10. AVAILABILITY/LIMITATION NOTICES: Enter any limitations on further dissemination of the report, other than those imposed by security classification, using standard statements such as:

(1) "Qualified requesters may obtain copies of this report from DDC."

(2) "Foreign announcement and dissemination of this report by DDC is not authorized."

(3) "U. S. Government agencies may obtain copies of this report directly from DDC. Other qualified DDC users shall request through _____."

(4) "U. S. military agencies may obtain copies of this report directly from DDC. Other qualified users shall request through _____."

(5) "All distribution of this report is controlled. Qualified DDC users shall request through _____."

If the report has been furnished to the Office of Technical Services, Department of Commerce, for sale to the public, indicate this fact and enter the price, if known.

11. SUPPLEMENTARY NOTES: Use for additional explanatory notes.

12. SPONSORING MILITARY ACTIVITY: Enter the name of the departmental project office or laboratory sponsoring *(paying for)* the research and development. Include address.

13. ABSTRACT: Enter an abstract giving a brief and factual summary of the document indicative of the report, even though it may also appear elsewhere in the body of the technical report. If additional space is required, a continuation sheet shall be attached.

It is highly desirable that the abstract of classified reports be unclassified. Each paragraph of the abstract shall end with an indication of the military security classification of the information in the paragraph, represented as *(TS), (S), (C), or (U)*

There is no limitation on the length of the abstract. However, the suggested length is from 150 to 225 words.

14. KEY WORDS: Key words are technically meaningful terms or short phrases that characterize a report and may be used as index entries for cataloging the report. Key words must be selected so that no security classification is required. Identifiers, such as equipment model designation, trade name, military project code name, geographic location, may be used as key words but will be followed by an indication of technical context. The assignment of links, rules, and weights is optional.